External Scintigraphy in Monitoring the Behavior of Pharmaceutical Formulations *In Vivo* I: Technique for Acquiring High-Resolution Images of Tablets

MICHAEL C. THEODORAKIS *§x, DAVID R. SIMPSON *, DOMINIC M. LEUNG *, and MICHAEL DEVOUS, Sr. *‡

Received February 18, 1981, from the *University of Illinois at Urbana-Champaign, *Section of Nuclear Medicine and Radiopharmacology and ‡Department of Bioengineering, Colleges of Veterinary Medicine and Engineering, Urbana, IL 61801.* Accepted for publication March 16, 1982. §Present address: College of Pharmacy, Department of Pharmaceutics, University of Florida, Gainesville, FL 32610.

Abstract □ A new method for monitoring tablet disintegration *in vivo* was developed. In this method, the tablets were labeled with a short-lived radionuclide, technetium 99m, and monitored by a gamma camera. Several innovations were introduced with this method. First, computer reconstruction algorithms were used to enhance the scintigraphic images of the disintegrating tablet *in vivo*. Second, the use of a four-pinhole collimator to acquire multiple views of the tablet resulted in high count rates and reduced acquisition times of the scintigraphic images. Third, the magnification of the scintigraphic images achieved by pinhole collimation led to significant improvement in resolution. Fourth, the radioinuclide was incorporated into the granulation so that the whole mass of the tablet was uniformly labeled with high levels of activity. This technique allowed the continuous monitoring of the disintegration process of tablets *in vivo* in experimental animals. Multiple pinhole collimation and the labeling process permitted the acquisition of quality scintigraphic images of the labeled tablet every 30 sec. The resolution of the method was tested *in vitro* and *in vivo*.

Keyphrases □ Disintegration—external scintigraphy in monitoring the behavior of pharmaceutical formulations *in vivo*, technique for acquiring high-resolution images of tablets □ Tablet formulation—external scintigraphy in monitoring the behavior *in vivo*, technique for acquiring high-resolution images of tablets □ Scintigraphy—external, monitoring the behavior of pharmaceutical formulations *in vivo*, technique for acquiring high-resolution images of tablets □ Radionuclides—^{99m}Tc-labeled tablets, external scintigraphy in monitoring the behavior of pharmaceutical formulations *in vivo*, technique for acquiring high-resolution images of tablets

Several techniques have been developed that permit the direct observation *in vivo* of pharmaceutical formulations such as tablets and capsules. The advantages and shortcomings of these techniques have been reviewed in a number of reports (1–3). Although at the present time the pharmaceutical scientists evaluate the formulation work by *in vitro* disintegration and dissolution studies coupled with *in vivo* blood studies, there are instances where the formulations of locally acting chemotherapeutic agents, antibiotics, antacids, and endogenous substances such as iron, potassium, and calcium salts do not provide distinguishable blood levels. Therefore, in such cases it is necessary to observe the *in vivo* disintegration time of the formulation in order to confirm the *in vitro* findings (2, 4). Furthermore, questions regarding the site of disintegration in the GI tract, the completeness of disintegration, the effectiveness of different enteric coatings, the rate of transition of the formulation through the different segments of the GI tract with respect to the age of the individual, the gastric and intestinal malfunctions, and diseases can be only answered by direct observation of the formulation within the GI tract. However, examination of the scientific literature during the last 50 years has revealed that only limited information is available on disintegration of formulations *in vivo*. This can be attributed to the fact that the previous techniques were difficult to perform and were invasive to both animal and human subjects. The development of the gamma scintillation camera coupled with the availability of short-lived gamma-ray emitting nuclides and devices for fast acquisition, processing, and storage of digital data has provided an opportunity to develop a useful method for performing such *in vivo* studies on tablets or capsules (3, 5–8). Furthermore, the development of mathematical methods of image reconstruction and enhancement of objects emitting gamma radiation has made it possible to enhance the resolution of the images of small objects acquired by the gamma scintillation camera (5, 6, 9).

The present report addresses further the application of external scintigraphy and image reconstruction in the acquisition of high-resolution scintigraphic images of labeled tablets *in vitro* and *in vivo*.

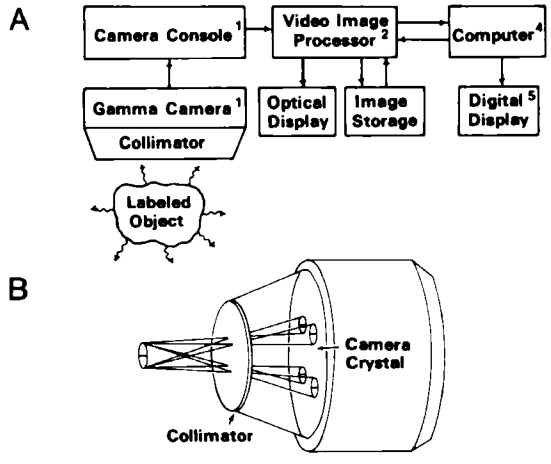

Figure 1—*(A) Block diagram of the image acquisition and data processing system; (B) projection of the four images using a four-pinhole collimator.*

EXPERIMENTAL

Image Acquisition and Processing—A standard gamma camera[1] with a sodium iodide–thallium iodide crystal (diameter 25.4 cm; thickness 1.25 cm) optically connected to 19 photomultiplier tubes was used to acquire the scintigraphic images of the labeled tablet phantoms and tablets *in vitro* and *in vivo*. The images were digitized and stored on magnetic tape[2] of the video image processor[3] prior to transmission to another computer[4] where the four pinhole images were back-projected

[1] Pho Gamma/HP, Siemens Gammasonics (formerly Searle Radiographics), Des Plaines, Ill.
[2] Primus, 9-Track Magnetic Tape, 9 in Reel, Wabash Tape Co., Huntley, Ill.
[3] Video Image Processor 460 (VIP-460), Technicare Inc. (formerly Ohio-Nuclear), Solon, Ohio.
[4] Eclipse S/140, Data General Corp., Southboro, Mass.

0022-3549/83/0200-0130$01.00/0

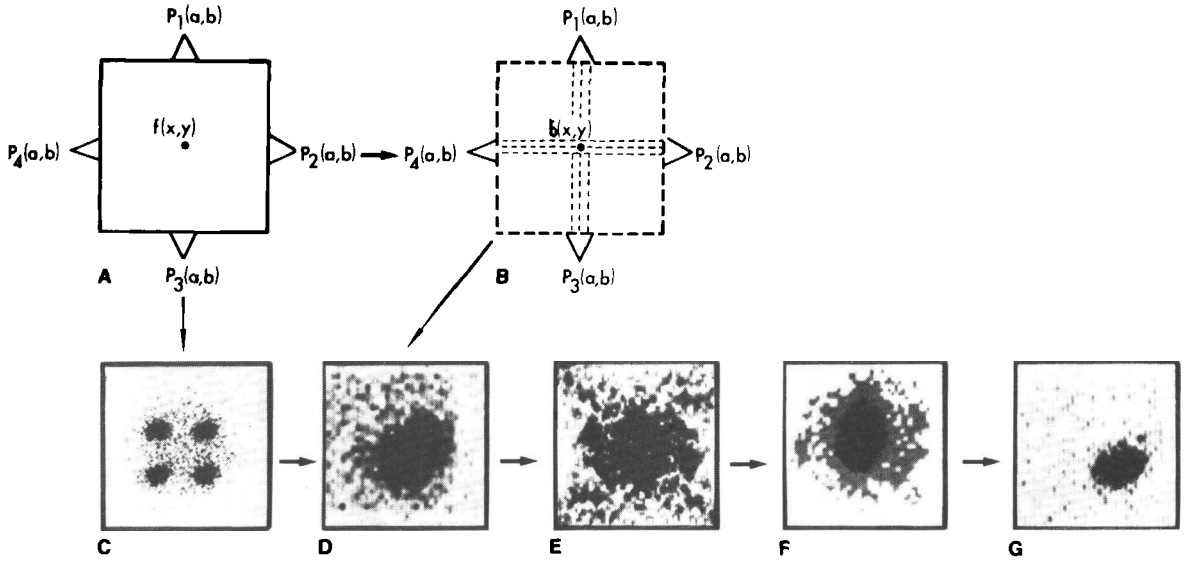

Figure 2—*Schematic illustration of the back-projection process (A and B) and the actual images of the back-projection and Fourier enhancement of a ^{99m}Tc-labeled tablet (C–G). (A) Four projections (images), $P_i(a,b)$, of a ^{99m}Tc-labeled tablet, f(x,y); (B) the images are back projected to form the back-projected image of the tablet, b(x,y); (C) original images, $P_i(a,b)$, of a tablet from a four-pinhole collimator; (D) back-projected image of the tablet, b(x,y); (E) Fourier spectrum of back-projected image of the tablet; (F) Fourier spectrum of the tablet's back-projected image after filtering the very high frequency components (noise); and (G) the enhanced back-projected image of the tablet after inverse Fourier transformation was applied on F.*

into one image which was enhanced by using filtered back-projection (Figs. 1B and 2). The final image was either displayed on the CRT screen of the video image processor, which also has photographic capability, or printed on a printer[5] using a 32-level gray scale display. The different interfaced devices and the flow of data are shown as a block diagram in Fig. 1A. A four-pinhole collimator was used to acquire four images of the labeled object. The distance between tablet and camera was optimized to provide the maximum magnification while all four images remained within the field of view of the camera. Serial images of the tablet were recorded at 30-sec intervals on the video image processor. The duration of data acquisition for each image was 30 sec.

Pinhole Collimator—A pinhole collimator was used to magnify and create four images of the tablet phantoms. The detachable pinhole assembly of a standard single-pinhole collimator was replaced by a lead cap of uniform thickness (0.3 cm) bearing four pinholes 0.119 cm in diameter, equally spaced on the periphery of a circle 3.8 cm in diameter (Figs. 1B and 3).

Pinhole Collimator Optimization—The diameter of the pinholes was optimized by imaging a ^{99m}Tc-labeled tablet (0.4 mCi). Images were taken with the tablet placed flat under the collimator and with the tablet placed on its edge. The counting time needed to accumulate 50,000 counts was plotted *versus* the pinhole diameter (Fig. 4).

Labeling of Tablets and Tablet Phantoms—Sodium [^{99m}Tc]pertechnetate (I) in saline (10 mCi/ml) received from a molybdenum-99–technetium-99m generator[6] was sprayed on the tablet granulation. The granulation was mixed, dried, and compressed[7] in tablets of specified hardness. Each tablet was labeled with 50,000–500,000 cpm as determined by the gamma camera detector. The diameter of the tablet was 1.04 cm and the thickness was 0.40 cm.

Five tablet phantoms were made of leather (Fig. 5A). Each phantom has a diameter of 0.8 cm and a thickness of 0.3 cm. Defects representing 0–9.9% of the weight of the phantom were artificially created (Table I). The phantoms were labeled by exposure to an aqueous solution of I. Each phantom was labeled with 100,000–200,000 cpm as determined by the gamma camera detector.

Back-Projection—The four images of the labeled phantom were back-projected into a single image by the following process. The distance between phantom and collimator was determined either by direct measurement or by the displacement of the images on the gamma camera crystal. This constant was used to determine the location of the four images on the crystal of the gamma camera. Then a two-dimensional array consisting of 64 × 64 picture elements (pixels[8]) was established around the center of each image. The four arrays were added together to form the back-projection image (Figs. 2A and B). The flow chart of the computer program used in back-projection is shown in Fig. 6A.

Image Enhancement—Pixels in the back-projected image were transformed into the Fourier domain first by rows then by columns, filtered (as will be described) and retransformed to the spatial domain. Image enhancement was completed when every pixel of the back-projected image was filtered. An example is given in Fig. 2. The flow chart of the computer algorithms used is shown in Fig. 6B.

Filter Optimization—To enhance the edges of the tablet and therefore increase the resolution, a modified ramp frequency filter[9] was used to filter the back-projected image of the tablet. This modified ramp frequency filter was derived by multiplying a basic ramp frequency filter with different frequency filters[9]. Several filters were constructed (Fig. 7). The best modified ramp frequency filter[9] was selected by evaluating the image–noise ratio (Table II). The image–noise ratio was established

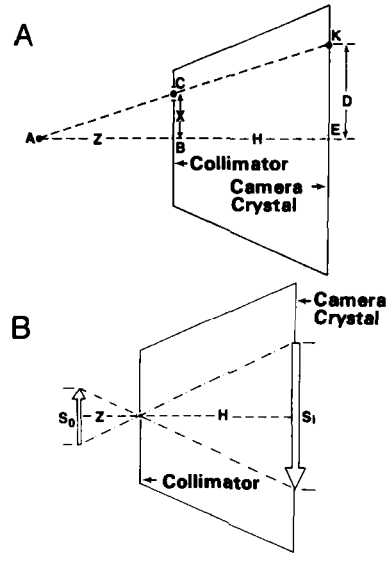

Figure 3—*(A) The location of the image (K) of tablet A, at distance D from the center of the gamma camera's sodium iodide–thallium iodide crystal was determined by the use of similar triangles ABC and AEK; (B) demonstration of image magnification and inversion by pinhole imaging.*

[5] Decwriter III, Digital Equipment, Marlboro, Mass.
[6] Mallinckrodt Nuclear Co., St. Louis, Mo.
[7] Hydraulic Press, model C, Fred S. Carver, Inc., Menomonee Falls, Wis.
[8] Pixel is an acronym for picture element.
[9] Butterworth.

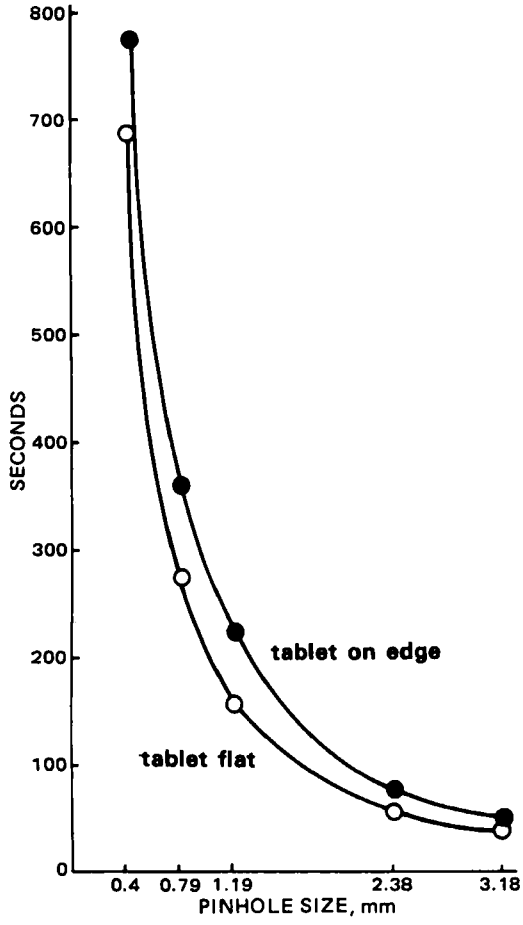

Figure 4—*Relationship between counting time and pinhole size.*

by dividing the number of counts in the pixels of the back-projected image of phantom tablet 1 (Fig. 5A) by the number of counts in an equal number of pixels in the background. The same frequency ramp filter was also evaluated in terms of image–defect ratio, which was established by dividing the average of the number of counts in the pixels corresponding to three intact portions, a, b, c, of the phantom tablet by the number of counts in the pixels corresponding to the defective area, d, of the tablet phantom 5 (Figs. 5A and B). All four areas, a, b, c, d, had an equal number of pixels.

Sensitivity to Defect Size—The labeled tablet phantoms, 2–5, were placed at different distances from the collimator, and their images were acquired and enhanced. The image–defect ratio was calculated for each defective phantom at different distances (Fig. 8). The image–defect ratio was used as a measure of evaluating the resolution of the technique with regard to the defect size of the tablet phantom and its distance from the collimator.

***In Vitro* Imaging Studies**—The *in vitro* imaging studies involved two parts. In the first part, ^{99m}Tc-labeled intact or defective tablet phantoms (Fig. 5A) were placed 6 cm in front of the collimator of the

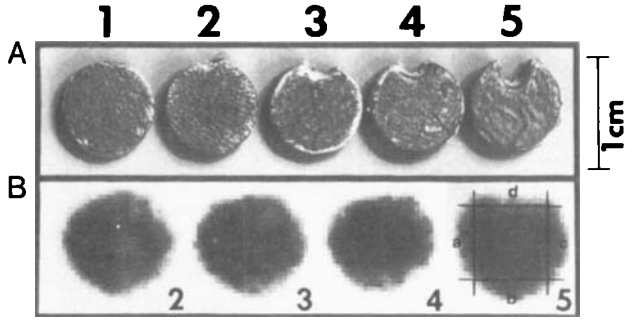

Figure 5—*(A) Tablet phantoms with various defects. (B) Enhanced scintigraphic images of the tablet phantoms with various size defects magnified five times by computer. Scale applies only to tablet phantoms.*

Table I—Size of Defects in Tablet Phantoms

Phantom No.	A[a], mm^2	B[b], %
1	0.0	0.0
2	0.62	1.2
3	1.4	2.8
4	2.6	5.2
5	5.0	9.9

[a] A is the area of defect in square millimeters. [b] B is the defect size expressed as the percent of the total weight of the phantom.

gamma camera and their images were acquired and reconstructed (Fig. 5B) according to the process described previously. The second part involved ^{99m}Tc-labeled tablets which were left to disintegrate in a shallow dish covered with distilled water. The water was lightly agitated occasionally. Scintigraphic images as well as photographs of the disintegrating tablet were taken every 30 sec (Fig. 9). The acquired images were reconstructed and enhanced.

***In Vivo* Imaging Studies**—The labeled tablet was administered orally to a dog weighing 13 kg. The animal was tranquilized[10] for imaging, placed in a supine position on a table, and the abdomen then was positioned under the collimated detector of the gamma camera. Data were accumulated for up to 75 min. During that period, scintigraphic images of the abdominal area were taken, back-projected, and enhanced (Fig. 10).

RESULTS

The acquisition and processing of the scintigraphic images are illustrated in Fig. 1A. The signal from the gamma camera console to the video image processor consisted of an x,y grid location of each detected emission within the specified energy range. Each of the images was digitized into a matrix of 64 × 64 pixels and stored on magnetic tape. The digitized images were transmitted to a general purpose computer[4] (16 bit, 512K) where the back projection and filtering of the scintigraphic image was conducted. The enhanced image was then displayed on the video image processor. The flow charts of the algorithms used for back-projecting and filtering the scintigraphic images are illustrated in Fig. 6.

The optimum diameter of the pinhole was determined experimentally by plotting the time needed to acquire 50,000 cpm from a ^{99m}Tc-labeled tablet *versus* the pinhole diameter size (Fig. 4). The optimum diameter was chosen to be 0.119 cm. The four pinholes were arranged equidistantly on the periphery of a cycle with a 3.8-cm diameter. The diameter was determined by using Eq. A1 (see *Appendix*) which was derived by geometric consideration of Fig. 3A. Distance (H) was constant at 16.7 cm. When a ^{99m}Tc-labeled tablet or tablet phantom placed at distance (Z) ranging from 3.3 to 7.5 cm, the image (K) was formed 11.5 and 6.1 cm from the center (E) of the crystal. The magnification was determined by Eq. A2, which was also derived by geometric consideration of Fig. 3. For instance, a tablet phantom with a 0.8-cm diameter placed 3.3 cm away from the collimator was magnified five times.

The back-projected image, $b(x,y)$, was in a sense the sum of the four images, $P_i(a,b)$, of the labeled tablet, $f(x,y)$, which were created by the four-pinhole collimator (Figs. 2A, B, and C). This back-projected image contained the true image in a single plane, and it was marked by interference due to natural background radioactivity, loss of small amounts of radioactivity because of the disintegration and dissolution process, and electronic noise (Fig. 2D). Each row and column of the 4096 pixel matrix (64 × 64) of each back-projected image was transformed from the spatial domain to the frequency domain by means of a Fourier transformation (Eq. A4). This is shown in Fig. 2E. The resulting frequencies from each column and row of pixels were filtered by the use of a modified ramp frequency filter[9], $f(k_x,k_y)$, which had been optimized experimentally (Eq. A5). The use of a frequency filter in the Fourier domain improved the image created by the process of back-projection by minimizing the very high-frequency components which were associated with the background interference and yet enchanced the frequency component of the back-projected image corresponding to the edges of the tablet. Each point of the filtered Fourier frequency spectrum (Fig. 2F) was transformed back to the spatial domain by means of an inverse Fourier transformation (Eq. A6), and the enhanced image of the tablet was obtained (Fig. 2G).

The modified ramp frequency filter[9], $f(k_x,k_y)$ (Eq. A5), was constructed by multiplying the relative magnitude of the ramp filter with the relative magnitude of another filter[9] at the same distance from the

[10] Rompun (Xylazine), 1.1 mg/kg, Bagvet, Division of Cutter Laboratories, Shawnee, Kan.

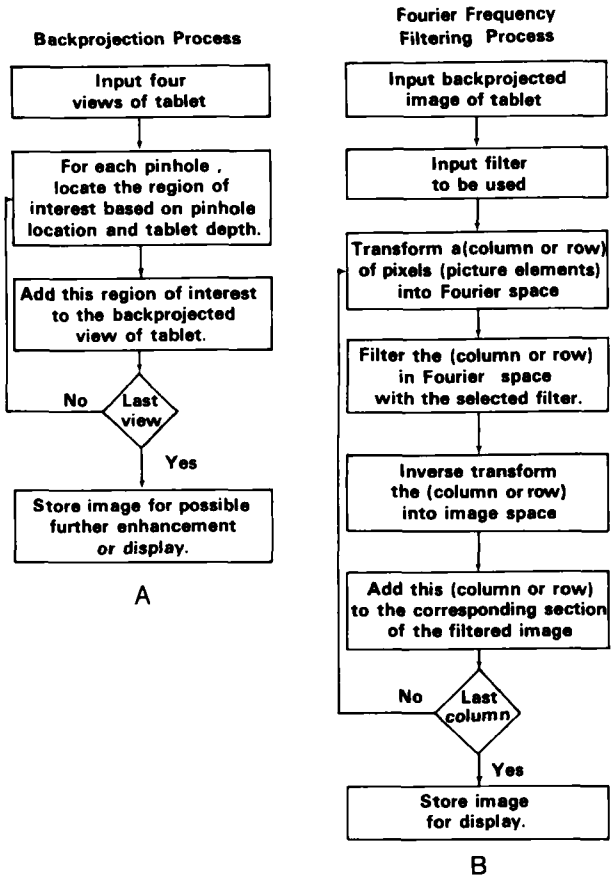

Figure 6—*Flow charts of the computer programs for back-projection (A) and for the filtering process (B).*

origin in the Fourier domain (Fig. 7). Several modified ramp frequency filters were used to enhance the images of the ^{99m}Tc-labeled tablets and tablet phantoms (Fig. 7). The image–noise ratio increased from filter 2 to 5 and then decreased gradually; on the other hand, the image–defect ratio declined rapidly from filter 2 to 5 and then leveled off (Table II). Frequency filter 3 (Fig. 7) was chosen for image enhancement and reconstruction as a reasonable compromise between image–noise and image–defect ratios.

The resolution of the method was tested *in vitro* by imaging a series of ^{99m}Tc-labeled tablet phantoms bearing artificial defects on the periphery (Fig. 5A). The labeled tablet phantoms were imaged at different distances from the collimator and the image–defect ratio was calculated (Fig. 8). When the image–defect ratio was ≥5, the defect was visible in the reconstructed image. The 0.62-mm^2 defect could not be resolved because it was smaller than the area of the pinhole (1.11 mm^2). Defect sizes as small as 1.42 mm^2 were discernible at a distance of 4.0 cm from the collimator. As the distance from the collimator increased and the magnification decreased, the resolution decreased rapidly (Fig. 8). For larger defects (5 mm^2), the resolution was independent of the magnification for distances ranging from 3.3 to 7.5 cm. The filtered back-projected images of each phantom are illustrated in Fig. 5B.

The resolution of the method was further tested *in vitro* with a series of experiments in which a rapidly disintegrating tablet labeled with

Table II—Image–Noise and Image–Defect Ratios for Various Frequency Filters

Filter	Image–Noise	Image–Defect
1	87.8	39.9
2	151.0	33.7
3	246.0	21.0
4	264.0	14.6
5	252.0	11.7
6 ramp filter	238.0	10.2
7	233.0	9.77
8	228.0	9.37
9	225.0	9.15
10	224.0	9.02

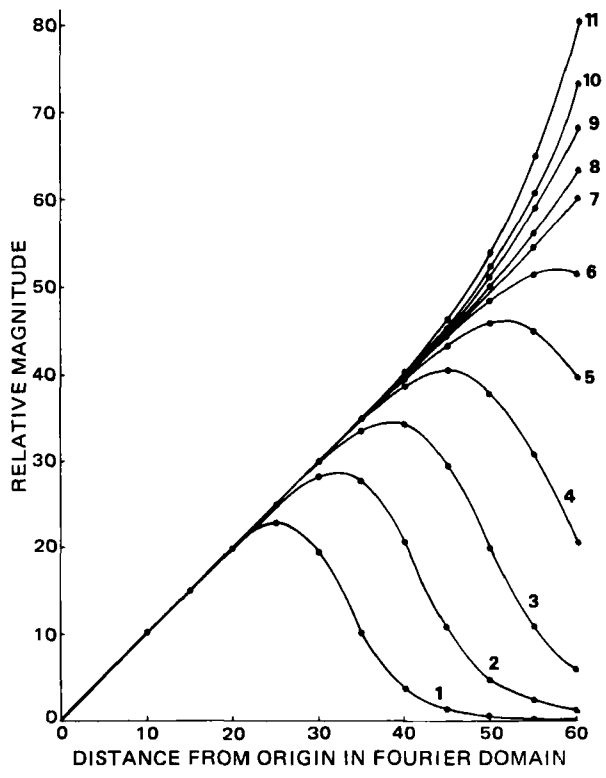

Figure 7—*Modified ramp frequency filters tested.*

technetium-99m was monitored with a gamma camera. The acquired scintigraphic images were processed and compared with photographs of the disintegrating tablet taken simultaneously with the images (Fig. 9). The disintegration started at 120 sec after the labeled tablet came in contact with the water and terminated 300 sec later (Fig. 9A). The scintigraphic images showed that the onset of the disintegration process was 180 sec after contact with the water (Fig. 9C).

The resolution of the technique was tested *in vivo* in the dog (Fig. 10). From the scintigraphs of the unprocessed image (Fig. 10A) and the corresponding back-projected and enhanced images (Fig. 10B), the onset of disintegration was evident 30 min postingestion, while at 75 min postingestion the tablet had undergone extensive disintegration.

DISCUSSION

The size of the pinhole was chosen to be 0.119 cm which was a compromise between the desired counting time (<60 sec) for a tablet labeled with 0.4 mCi of technetium-99m and the desired resolution which cannot be smaller than the diameter of the pinhole itself (10). The counting time was inversely proportional to the square of the radius of the pinhole and proportional to the square of the distance between labeled tablet and the collimator.

The spacing of the pinholes on the collimator was also critical. If the pinholes were very close together, then the four images formed on the camera crystal overlapped as the labeled tablet moved away from the camera. However, if the pinholes were spaced far apart, then the images were formed outside of the crystal as the labeled tablet moved closer to the collimator. Therefore, with an established pinhole size of 0.119 cm in diameter as optimum and with the equidistant spatial arrangement of the four pinholes on a circle 3.8 cm in diameter, the imaging of a tablet was feasible in distances ranging from 3.3 to 7.5 cm away from the collimator. The advantage of using a four-pinhole collimator was that four images were collected simultaneously. This increased the efficiency of detection by increasing the total counts collected in a certain time or by decreasing the time needed to acquire an image with a certain number of counts. In turn, short times of image acquisition minimized the effect of the slight perturbations of the tablet due to GI motility. Also, the interference of background was reduced by increasing the count rate. Finally, the pinhole magnified the image thereby improving the resolution (Fig. 3B).

The back-projection process (Figs. 2A–D) made the use of the four-pinhole collimator beneficial, while the process of Fourier enhancement (Figs. 2E–G) improved the resolution by eliminating the high-frequency

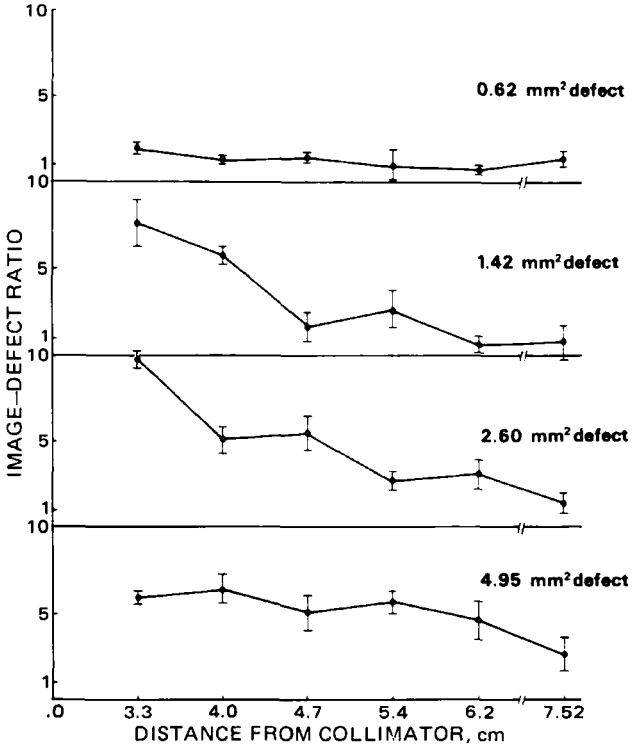

Figure 8—*The image-defect ratio as a function of distance and defect size. Image-defect ratio, larger than five yields observable defects.*

components (interference) of the back-projected image (Fig. 2). The reconstructed image (Fig. 2G) had more sharply defined edges than the back-projected image (Fig. 2D).

The resolution of the technique depended on the size of the pinhole diameter (10) and the type of frequency filter used to filter the Fourier spectrum of the back-projected image of the tablet (Figs. 2E and F). Every pixel of the back-projected image was transformed from the spatial domain to the frequency domain by Eq. A4, and then the modified ramp frequency filter was applied to eliminate the background interference and sharpen the edges of the tablet (Eq. A5). The image-noise and image-defect ratios (Table II) are a good measure for testing the resolution of the technique and selecting the optimum modified ramp frequency filter from other alternatives (Fig. 7). Defects of 5 mm^2 were readily recognizable at distances ranging from 3.3 to 7.5 cm. The *in vitro* experiments using ^{99m}Tc-labeled tablets with a 1.04-cm diameter showed that the resolution was improved by the enhancement process and the onset of disintegration became evident 60 sec after the process had started (Fig. 9). In the *in vivo* experiments, the onset of disintegration became evident ~30 min postingestion. This was because the resolution was compromised due to the interference of the abdominal and stomach tissue; therefore, the observable defect was probably >5 mm^2. The disintegration *in vivo* was slower than *in vitro*, thus, confirming observations of previous investigators (11).

The incorporation of the radioisotope, technetium-99m, into the tablet granulation in the form of spray of a saline solution of I ensured the uniform distribution of the label throughout the entire mass of the tablet. This method of labeling gave better results than a previously reported method where the labeling was achieved by exposing the tablet itself to vapors of iodine-131 (3). In that method, the surface of the tablet was uniformly coated with iodine-131; however, the penetration of the label into the core was inadequate. The mass of I that was incorporated into the tablet was negligible (~10^{-11} g of I/tablet), and, therefore, the physical or chemical integrity or characteristics of the formulation remained unaffected. The radioactivity of the labeled tablets ranged from 50,000 to 500,000 cpm/tablet. Finally, in instances where the formulation is sensitive to moisture, the technetium-99m can be added in the form of a dry powder derived by lyophilization of a solution of I in saline or [^{99m}Tc]-methylene disphosphonate in saline.

The technique of external scintigraphy has been applied before for the purpose of monitoring the disintegration *in vivo* of tablets and capsules (3, 7, 8). However, in both instances the technique did not involve enhancement of the scintigraphic images, and thus, the detection of small defects that would signify the onset of the disintegration process could

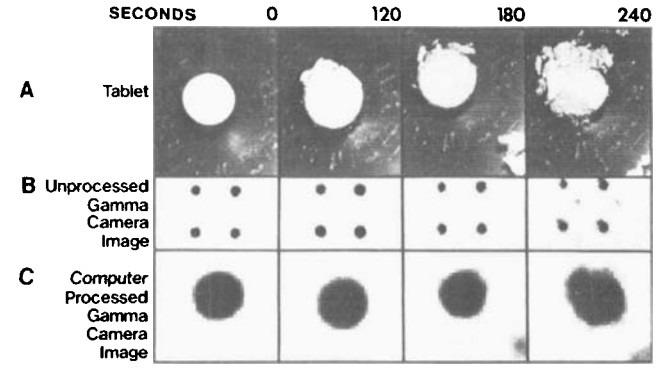

Figure 9—*Photographs (A) and* in vitro *scintigraphic images of a ^{99m}Tc-labeled tablet before (B) and after enhancement (C).*

not be evidenced due to the lower resolution of the technique. On the other hand, the present technique, which combines external scintigraphy with image enhancement, increased the resolution of the system so that small defects on the formulation can be detected, and it reduced the interference of the background activity, which may be attributed either to natural radioactivity, dissolution of the label to the dispersal of the fine labeled granules, or to a combination of these factors. This reduction of the background interference facilitates the monitoring of disintegration of small fragments of the formulation and, thus, enables the observer to determine the end of the disintegration process. Furthermore, reduction of the background interference will be useful when the determination of the transition times of the disintegrating formulation through the GI tract will be attempted, especially at the stages where considerable portions of the formulation have disintegrated.

A similar technique which also involved labeling of the formulation with gamma ray emitters such as iron-59, technetium-99m or chromium 51 and made use of two simple sodium iodide–thallium iodide crystal detectors has been applied in evaluating the disintegration and dissolution of tablets and capsules *in vivo* (4, 12). However, this technique did not allow direct observation of the formulation; thus, the onset and end of the disintegration *in vivo* could not be determined with any reasonable accuracy.

In the past, most of the techniques that were developed for determining the disintegration time of tablets *in vivo* were based on the use of roentgenography or fluoroscopy with or without the inclusion of radiopaque materials in the formulation (1, 2, 11, 13). Those techniques exposed the animal or human subject to high radiation doses of X-rays; they did not allow magnification or enhancement of the tablet's image; they could not be used for continuous monitoring of the formulation in the GI tract; and finally, rendering a nonradiopaque formulation radiopaque required inclusion of large amounts of radiopaque substances relative to the mass of the formulation, thus, effectively altering the composition of the formulation. In contrast, the proposed technique is free of the aforementioned shortcomings. The main feature of this method is the high resolution. The high resolution was achieved by using a four-pinhole collimator, which magnified the four scintigraphic images of the labeled tablet phantom or tablet, and by image enhancement of the back-projected image using Fourier transformation and filtering.

APPENDIX

Initial testing of image reconstruction and enhancement algorithms were performed with scintigraphic images of tablet phantoms. The method of image acquisition and enhancement applied in this study involved three separate steps. First, the determination of the location of the four pinhole projections of the tablet phantom on the crystal of the gamma camera; second, the back-projection of the four projected images to form a single back-projected image; and third, the enhancement of the back-projected image using filtering techniques based on Fourier transformations.

The determination of the location of the phantom's images on the crystal of the gamma camera involved simple Euclidean geometry (Fig. 3A). The displacement D of the tablet's image K from the center of the camera crystal is given by:

$$D/(Z + H) \approx X/Z \qquad \text{(Eq. A1)}$$

where Z is the distance from center of the collimator to tablet A, H is the distance from center of the collimator to the center of camera crystal (16.7

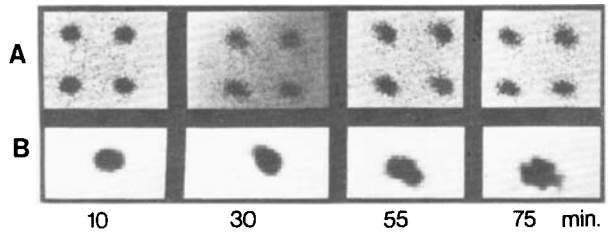

Figure 10—*Scintigraphs of a disintegrating tablet* in vivo *before (A) and after processing (B).*

cm), and X is the distance from the center of the collimator to the pinhole (1.9 cm).

The image magnification (Fig. 3B) is given by the size relationship between tablet phantom, S_o, and its image S_i, described by:

$$S_o/S_i = Z/H \qquad \text{(Eq. A2)}$$

The four images (projections), $P_i(a,b)$, of the tablet phantom were then combined to form the back-projected image, $b(x,y)$. Mathematically, the process is described by:

$$b(x,y) = \sum_{i=1}^{m} P_i(a,b) \qquad \text{(Eq. A3)}$$

where $b(x,y)$ was a point in the back-projected image, $P_i(a,b)$ was the point on the ith image corresponding to $b(x,y)$, and m was the number of images obtained. The back-projection process is described diagrammatically in Figs. 2A and B. Four images (P_1–P_4) of the labeled tablet phantom $f(x,y)$ were taken (Fig. 2A). The four images were then combined (back-projected) to form the back-projected image, $b(x,y)$ (Fig. 2B). The back-projected image actually contained the true image of the labeled tablet which was masked by background interference (noise artifacts) during the process of back-projection (Fig. 2D).

The back-projected image of the tablet phantom was improved by frequency domain filtering using Fourier transformations. It was based on the fact that both edges and noise artifacts in the image were represented by very high frequencies when the image was transformed into the frequency domain. Thus, by transforming the image from its spatial domain into its frequency domain, filtering can be performed to enhance the edges and, at the same time, try to reduce the background interference by filtering out the very high-frequency components.

The process of frequency filtering of the back-projected image involved three steps. In the first step, each row and column of pixels in the image was transformed into the Fourier domain, $F(k_x k_y)$, by performing two-dimensional Fourier transformation as given by:

$$F(k_x,k_y) = \int_{-\infty}^{\infty}\int_{-\infty}^{\infty} b(x,y)\exp(-2_\pi i(k_x x + k_y y)dxdy) \qquad \text{(Eq. A4)}$$

where $b(x,y)$ is the back-projection image pixel values, k_x and k_y are variables representing distances from the origin in the Fourier domain, and $i = \sqrt{-1}$ (14, 15).

In the second step, each Fourier coefficient $F(k_x k_y)$ was multiplied by a modified ramp frequency filter[9] $f(k_x,k_y)$, and thereby converted to the Fourier coefficients $F_I(k_x,k_y)$ of the final image:

$$F_I(k_x,k_y) = F(k_x,k_y) \times f(k_x,k_y) \qquad \text{(Eq. A5)}$$

In the third step, the Fourier coefficients of the final image, $F_I(k_x,k_y)$, were transformed back to the spatial domain by application of the inverse Fourier transformation:

$$b'(x,y) = \int_{-\infty}^{\infty}\int_{-\infty}^{\infty} F_I(k_x,k_y)\exp(2_\pi i(k_x x + k_y y)dxdy) \qquad \text{(Eq. A6)}$$

where $b'(x,y)$ was the pixel value in the final image.

The process of Fourier transformation and filtering is shown in Figs. 2B, E, and F. In Fig. 2C the four images taken from the four-pinhole collimator are shown. The four images are then back-projected to form the back-projected image (Fig. 2D). Discrete Fourier transformation is performed on the image (Fig. 2E). The origin of the frequency domain is in the middle of the image. The components around the four corners represented random noise. The frequency domain was then filtered, and the filtered spectrum is shown in Fig. 2F. The very high-frequency components, which represent noise, are filtered out, and the high frequencies are enhanced. The filtered frequency domain is then transformed back to the spatial domain and the enhanced, back-projected image is shown in Fig. 2G.

REFERENCES

(1) J. G. Wagner, "Biopharmaceutics and Relevant Pharmacokinetics," 1st ed., Drug Intelligence Publications, Hamilton, Ill., 1971, p. 72.

(2) W. H. Steinberg, G. H. Frey, J. N. Masci, and H. H. Hutchins, *J. Pharm. Sci.*, **54**, 747 (1965).

(3) M. C. Theodorakis, M. D. Devous, Sr., and D. R. Simpson, *ibid.*, **69**, 1107 (1980).

(4) M. Alpsten, G. Ekenved, and L. Solvell, *Acta Pharm. Suec.*, **13**, 107 (1976).

(5) M. C. Theodorakis, M. D. Devous, Sr., and D. R. Simpson, "Abstracts," vol. 10, No. 1, APhA Academy of Pharmaceutical Sciences, Washington, D.C., 1980, p. 79.

(6) M. C. Theodorakis, M. D. Devous, Sr., and D. R. Simpson, in "Radionuclide Imaging in Drug Research," C. G. Wilson, J. G. Hardy, M. Frier, and S. S. Davis, Eds., Croom and Helm, Ltd., London, England, 1982, pp. 153–169.

(7) D. L. Casey, R. M. Beihn, G. A. Digenis, and M. B. Shambhu, *J. Pharm. Sci.*, **65**, 1412 (1976).

(8) G. A. Digenis, in "Radionuclide Imaging in Drug Research," C. G. Wilson, J. G. Hardy, M. Frier, and S. S. Davis, Eds., Croom and Helm, Ltd., London, England, 1982, pp. 103–143.

(9) R. A. Vogel, D. Kirch, M. LeFree, and P. Steele, *J. Nucl. Med.*, **19**, 648 (1978).

(10) W. L. Rogers, "Update on Multiple Pinhole Tomography," Third Annual Conference on Advances in Emission Tomography at Andover, Mass., October 1979.

(11) G. Levy, *J. Pharm. Sci.*, **52**, 1039 (1963).

(12) M. Alpsten, C. Bogentoft, G. Ekenved, and L. Solvell, *J. Pharm. Pharmacol.*, **31**, 480 (1979).

(13) J. G. Wagner, W. Veldkamp, and S. Long, *J. Am. Pharm. Assoc., Sci. Ed.*, **47**, 681 (1958).

(14) R. L. Gonzalez and P. Wintz, "Digital Image Processing," 1st ed., Addison-Wesley, Reading, Mass., 1979, p. 36.

(15) T. F. Budinger, *J. Nucl. Med.*, **21**, 579 (1980).

ACKNOWLEDGMENTS

Supported by Grant CA 09067 awarded by the National Cancer Institute, Department of Health, Education, and Welfare (Department of Health and Human Services).

Part of this work was presented at the annual meeting of the American Pharmaceutical Association in Washington, D.C. in April 1980, and at the 2nd International Symposium on "Applications of Radionuclides in Drug Formulation Studies," Department of Pharmacy, University of Nottingham, Nottingham, England, April 1–3, 1981.